


## Optimization of the Sunset Yellow dye removal by electrocoagulation using a response surface method

Mitra Afshar Moghaddam and Kambiz Seyyedi 

Department of Chemistry, Tabriz Branch, Islamic Azad University, Tabriz 5157944533, Iran

\*Corresponding author. E-mail: k.seyyedi@iaut.ac.ir

 KS, 0000-0002-9498-5255

### ABSTRACT

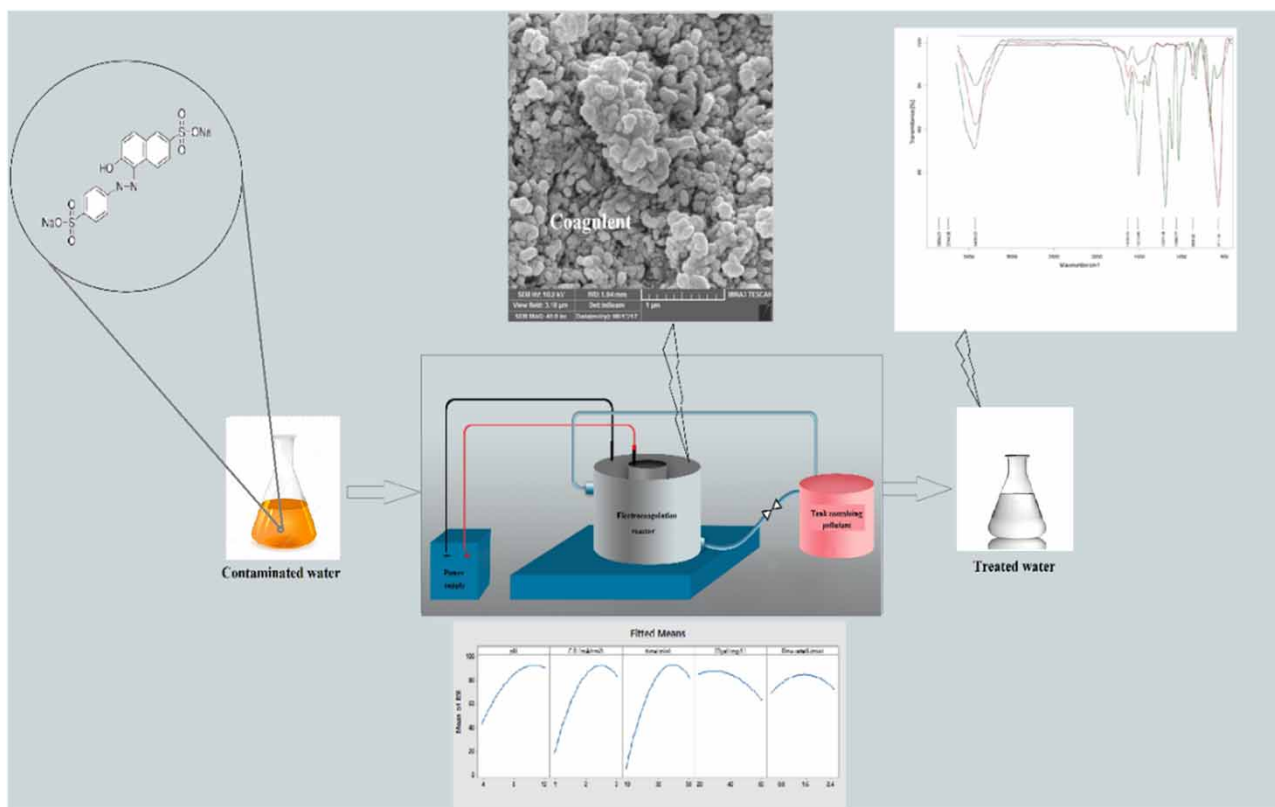
In recent years, among the various treatment methods, the electrocoagulation process has been used for the treatment of effluents containing various dye pollutants. Sunset Yellow (S.Y.) azo dye is one of the common food colors widely used in various food industries. This study investigated the removal of the dye S.Y. from aqueous media by the electrocoagulation method in an electrochemical reactor using concentric iron electrodes. The experiments were designed using the response surface method (RSM) with the help of Minitab software in such a way that the effect of various process-influencing parameters, such as current density, electrolysis time, electrolyte concentration, pH of the solution, and the effluent flow rate, on the desired pollutant removal efficiency was investigated. According to the results of the process optimization by RSM, the optimal conditions for the process were obtained as follows: pH of 10, current density of 2.65 mA/cm<sup>2</sup>, electrolysis time of 42.32 min, initial dye concentration of 20 mg/L, and effluent flow rate of 2.5 L/min. Under the above optimal conditions, the efficiency of dye removal was more than 99%.

**Key words:** concentric iron electrodes, dye removal efficiency, electrocoagulation, optimization, response surface methodology, Sunset Yellow

### HIGHLIGHTS

- Electrocoagulation is a very efficient process for removing dyes from contaminated waters.
- Response surface methodology approach is a very effective tool for optimizing the electrocoagulation process.
- Optimization of the electrocoagulation process reduces the use of chemicals and protects the environment.
- The electrochemical reactor using concentric electrodes is an appropriate reactor for treatment of wastewater.

## GRAPHICAL ABSTRACT



## INTRODUCTION

All natural waters contain a variety of pollutants that originate from the processes of erosion, washing, and contact with air. In addition to natural pollution, there are other pollutants that result from the discharge of domestic and industrial wastewater into the sea, the Earth's surface, the Earth's crust, or surface waters. Each volume of water is able to accept certain amounts of contamination through dilution and self-purification agents without serious complications. If the contamination rate increases, the nature of the receiving water changes, and its use for different purposes may not be appropriate. Understanding the effects of pollution and existing control facilities is very important in the effective management of water resources (Liu *et al.* 2021).

In industrial and domestic wastes, many substances, including various chemicals and industrial solvents, detergents, all kinds of drugs, dyes, and various materials, enter running waters or groundwaters. Among the various types of pollution, effluent flow is one of the biggest problems due to high water consumption in our daily lives. Dye-containing effluents are also a major source of water pollution. Dyes are discharged into the ecosystem, which causes deterioration of water quality, this influences plants and animals and causes chronic and severe toxicity, all of which are a potential hazard to human health. Some of the most important water pollutants are synthesized compounds such as dyes, which are widely used in food, dyeing, textile, paper, and plastic industries. The presence of organic pollutants such as dyes in surface and groundwaters is dangerous and undesirable. Some organic pollutants have been shown to be toxic, and some cause genetic mutations in aquatic organisms. The release of these polluted effluents into the ecosystem destroys nature and disrupts aquatic life. In addition, the stability of their molecular structure makes them resistant to biological or even chemical decomposition (Kashefialasl *et al.* 2005; Arnold *et al.* 2012). In this research, Sunset Yellow (S.Y.), which is from the azo color group, has been studied. This color is widely used in Iran's food industry, including the production of puffs, soft drinks, ice cream, jellies, pastilles, jams, ready-made soups, chocolates, and cakes (combined with other colors to produce the brown color in chocolates and desserts). Rarely, it causes allergic skin reactions, and in some people with asthma it

can make the symptoms worse. Likewise, the possibility of hyperactivity in children prone to this disorder has been investigated in one study, but no other confirmatory research is yet available (Gao *et al.* 2016; Deepika *et al.* 2017). The acceptable daily intake (ADI) of S.Y. is 0–4 mg/kg under both EU and WHO/FAO guidelines.

In recent years, various biological methods and physical and chemical processes such as precipitation, chemical coagulation, ion exchange, advanced oxidation processes, adsorption processes on activated carbon and various adsorbents, membrane processes such as nanofiltration, and reverse osmosis have been used for decolorization; however, each of them has its own advantages and disadvantages (Seyyedi & Mahdiyari 2015; Khadivi *et al.* 2019; Elami & Seyyedi 2020; Naresh Yadav *et al.* 2021). Among these efficient methods, we can refer to electrocoagulation, which is an easy and practical method with low cost, based on electrochemical methods, and does not require chemical additives (Sires & Brillas 2012; Syam Babu *et al.* 2020). Today, it is mainly used for the treatment of wastewaters produced in food and oil industries, dye and textile industries, and chemical and mechanical polishing. It has also been greatly useful in removing detergents and heavy metals from wastewater (Hanay & Hasar 2011; Gomes *et al.* 2016; Gautam *et al.* 2020; Bracher *et al.* 2021). Nippa-tlapalli & Philip (2020) reported that proper design of reactors helps to improve the efficiency of electrocoagulation process. In this study, the performance of the designed novel electrolytic reactor with a rotating bipolar multiple disc electrode (RBDE) in the electrocoagulation–flotation (EC-F) process and a pulsed plasma reactor for the removal of toxic textile dyes was evaluated. Reactive Blue 19 and Methyl Orange were completely decolorized (100%) within 2 min of electrolysis time with rotating and 6 min with static (nonrotating) electrodes, respectively. Xu *et al.* (2021) investigated the application of hybrid electrocoagulation–filtration methods in the pretreatment of marine aquaculture wastewater. They found that the EC–filtration system is effective for the removal of chemical oxygen demand (COD), total ammonia nitrogen (TAN), nitrite, nitrate and total nitrogen (TN) in aquaculture wastewater.

In this process, the removing agent of the pollutants (iron or aluminum hydroxide clots) is produced by the electrochemical reactions, which use an electrochemical cell (Khoshbin & Seyyedi 2017). Hence, wastewater treatment is conducted according to the following three major processes:

1. Electrochemical reaction on the surface of the electrode is followed by coagulant formation in the aqueous media.
2. The pollutants which are soluble or colloidal are adsorbed on coagulants.
3. Removing via sedimentation or floatation (Sahu *et al.* 2014; Lu *et al.* 2021).

If iron is used as an electrode, the following reactions are observed:

At the anode:



At the cathode:



Overall reaction:



The obtained  $\text{Fe}(\text{OH})_3$  stays in the aqueous solution in the form of a gelatinous suspension and can remove pollutions from wastewater by complexation or electrostatic attraction after which the coagulation phenomenon takes place. In the complex formation mechanism happening on the surface, the pollutants are attracted to the hydrated iron in the form of a ligand (Garajehdaghi & Seyyedi 2019). The sludge particles can be separated by electro-flotation when they are attached to the bubbles of  $\text{H}_2$  gas evolved at the cathode, being transported to the solution surface in the reactor where they can be withdrawn.

By the acquisition of the values of the output variables obtained from the experiments in the optimization stage, a regression function is performed. This regression function actually expresses the answer as a function of the variables in the experimental design. A fitting of the regression function, which is an estimate of the response of the system in question, leads to its optimization as the objective function, and the optimal values of the model variables are determined (Bendaia

*et al.* 2021). These steps are sequences used in response surface methodology for analyzing a problem. Central composite and Box–Behnken methods are the two main methods of response surface design. In recent years, the use of various experimental design methods, including the response surface method (RSM), is preferred over other factorial approaches since it can reduce the number of required tests by simultaneously reviewing their effects, resulting in time and cost savings (Mook *et al.* 2017; Ghaffarian Khorram & Fallah 2018; Chelladurai *et al.* 2021). The present study sought to investigate the feasibility of treating the sewage polluted with one of the most widely used food dyes in the food industry, S.Y. dye, by an electrochemical reactor using concentric iron electrodes. For this purpose, the effect of different parameters, such as the current density, electrolysis time, electrolyte concentration, pH of the solution, and effluent flow rate, was investigated, and the process optimization was probed by the RSM run in Minitab software.

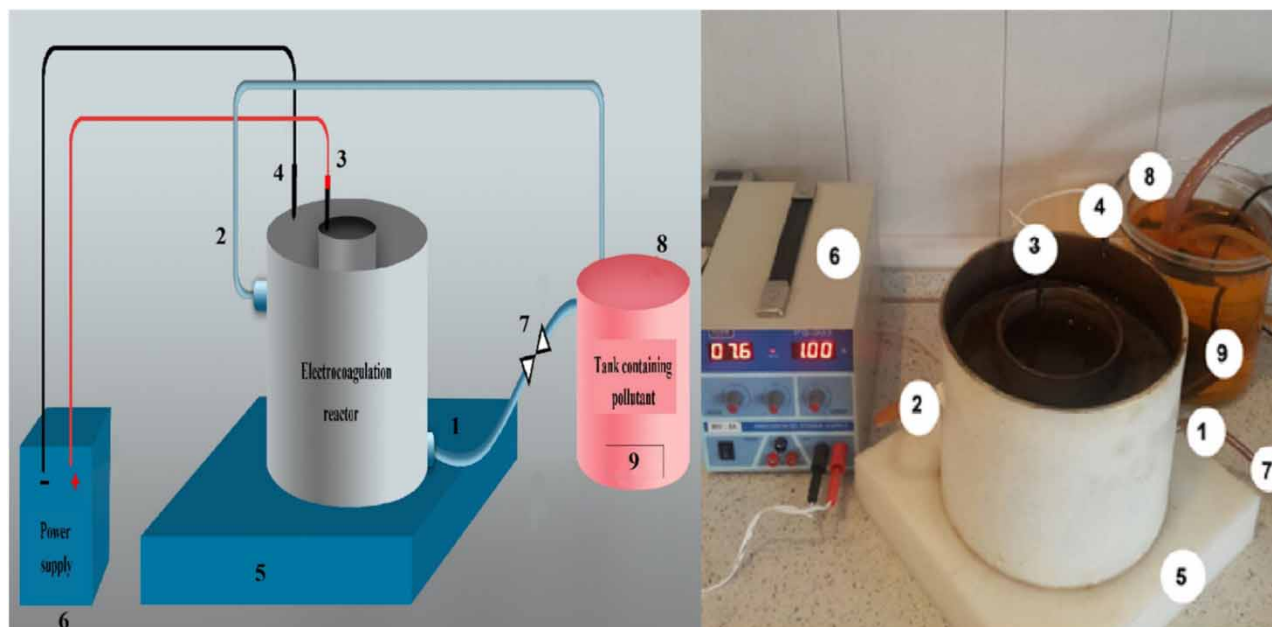
## MATERIALS AND METHODS

### Design of reactor

As shown in Figure 1, the electrocoagulation system consists of a power supply, DC anode and cathode electrodes, a reservoir to hold the solution or effluent, and, finally a pump to create a fluid flow inside the reactor. The used recirculating electrochemical reactor consists of an iron cylinder with a diameter of 21 cm, a height of 15 cm, and a thickness of 3 mm as the cathode, and another iron cylinder with a diameter of 11.4 cm and the same height and thickness as the anode. Both cylinders concentrically were fixed on a Teflon plate (as electrical insulation to prevent the connection of the anode and cathode). Eleven holes with a diameter of 1 cm were installed on the surface of the anode, enabling the entry of the solution to the space of the inner cylinder and electrolysis on the inner surface of the anode. The iron cylinders were designed and sized during construction in such a way that the anode surfaces were exactly the same size as the cathode surface. Similarly, the number and area of the embedded holes were adjusted by the calculation of these levels. Anode and cathode areas of  $691\text{ cm}^2$  were calculated and constructed.

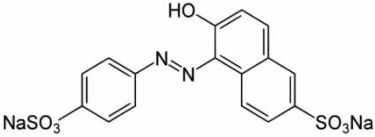
### Chemicals and the analysis

All the chemicals used in the study, including NaCl, NaOH, and HCl, were provided by the Merck Company, and the applied S.Y. dye was obtained from the Narmada Company (India- 87% purity). Table 1 lists the structure and characteristics of S.Y.



**Figure 1** | Electrochemical reactor with concentric electrodes used to remove Sunset Yellow dye by electrocoagulation method. (1) Solution input to reactor, (2) solution output from reactor, (3) positive pole connection of power supply to anode, (4) negative pole connection of power supply to cathode, (5) Teflon electrical insulation base, (6) power supply, (7) valve for regulating the flow rate of the solution to the reactor, (8) storage tank, (9) water pump.

**Table 1** | Chemical structure and characteristics of Sunset Yellow (S.Y.)

Chemical structure	
Chemical formula	$C_{16}H_{10}N_2O_7S_2Na_2$
IUPAC name	Disodium 6-hydroxy-5-[(4-sulfophenyl)azo]-2-naphthalenesulfonate
Color index	Food Yellow 3, Orange Yellow S
Color index number	C.I. 15985
Molecular weight	452.36 g/mol
Classification	Mono azo dye
CAS number	2783-94-0
Solubility in water (g/L)	120

As shown in Figure 1, the experiments were performed in the reactor at a temperature of about 297 K with 7 liters of the dye solution. To increase the electrical conductivity of the solution, sodium chloride was added at different concentrations as the electrolyte. A power supply (ADAK-PS808) was used for generating current and applying voltage. A pump was employed for creating fluid flow inside the reactor. In addition, sampling was performed at the appointed times. The sampled solution to separate the clots was immediately placed in a centrifuge (Hettich EBA20) at 4,000 rpm for 15 minutes. In order to evaluate the efficiency of the electrocoagulation method in the dye removal of S.Y., the absorbance of the solution was determined before and after electrolysis using a spectrophotometer (UNICO 2100) and the residual concentration of dye in the filtered solution was measured at  $\lambda_{max} = 482$  nm, using a calibration diagram. In order to evaluate the effect of pH of solution on the removal efficiency, and to adjust the pH level to desired value, 0.1 M HCl and NaOH solutions were used. The pH of the solution was measured using a pH meter (Metrohm). It should be noted that the reactor was washed with hydrochloric acid 0.1 M and then twice with water after each test and before the start of the next test. As in Table 2, to optimize the process, the experimental design was implemented using the central composite design method run in Minitab software (Version 17). In the experimental design method, the experiments are designed in such a way that the factors are tested simultaneously to obtain the answer. The main design framework of the experiment is based on a series of standard schemes that considers the interaction between factors in order to affect each other. In this case, the final optimal point can be reached with a smaller number of experiments.

The morphology of the sludge was evaluated using scanning electron microscopy (SEM) (CamScan, MV2300 instrument, Canada). Meanwhile, Fourier transform infrared (FTIR) (Bruker Tensor 27, Germany) and Brunauer–Emmett–Teller (BET) (Belsorp-mini 2, Japan) instruments were used to study the functional groups and surface properties of the sludge, respectively.

**Table 2** | Experimental design matrix for experimental and predicted S.Y. removal

Coded variables	Variable levels				
	-2	-1	0	+1	+2
pH ( $X_1$ )	4	6	8	10	12
Time (min) ( $X_2$ )	10	20	30	40	50
Current density (mA/cm <sup>2</sup> ) ( $X_3$ )	1	1.5	2	2.5	3
Dye concentration (mg/L) ( $X_4$ )	20	30	40	50	60
Flow rate (L/min) ( $X_5$ )	0.5	1	1.5	2	2.5

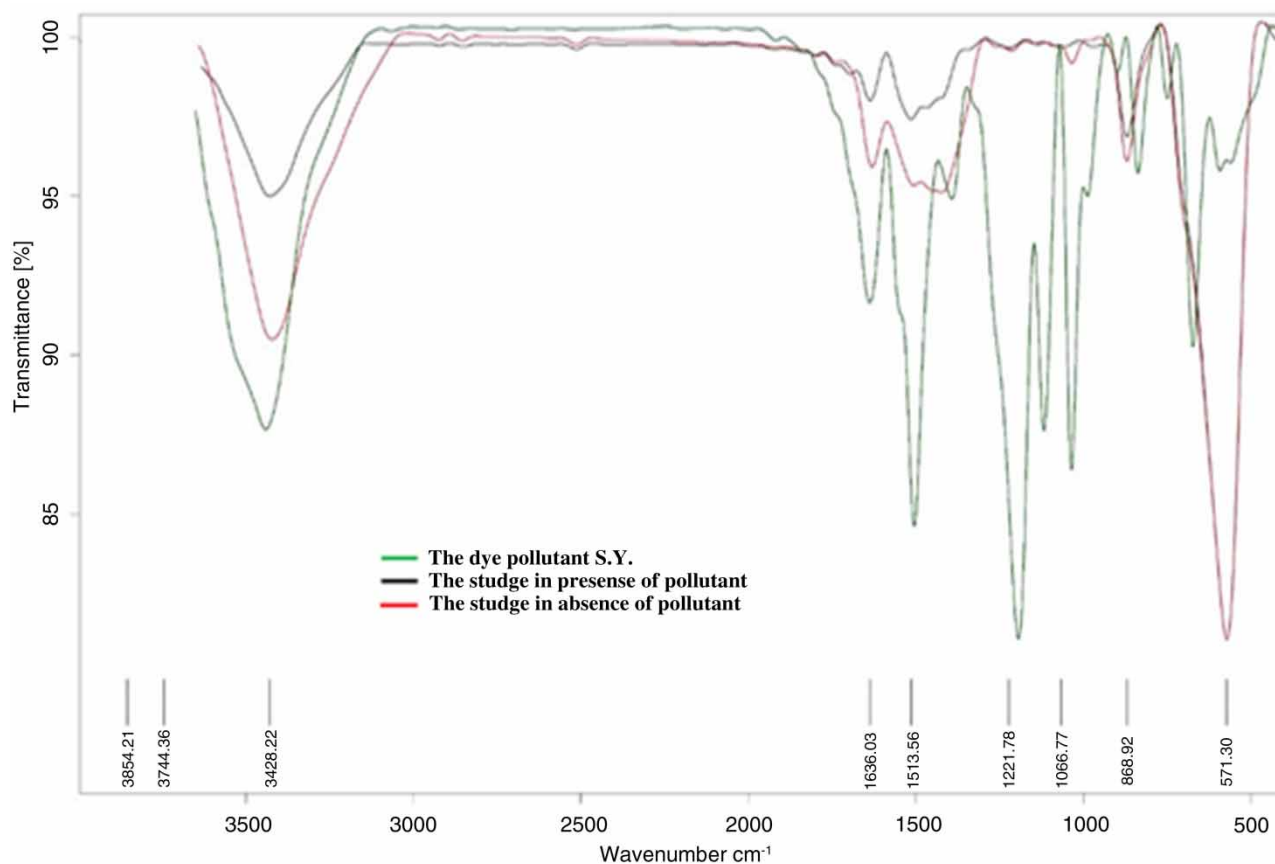
## RESULTS AND DISCUSSION

### FTIR spectroscopy study

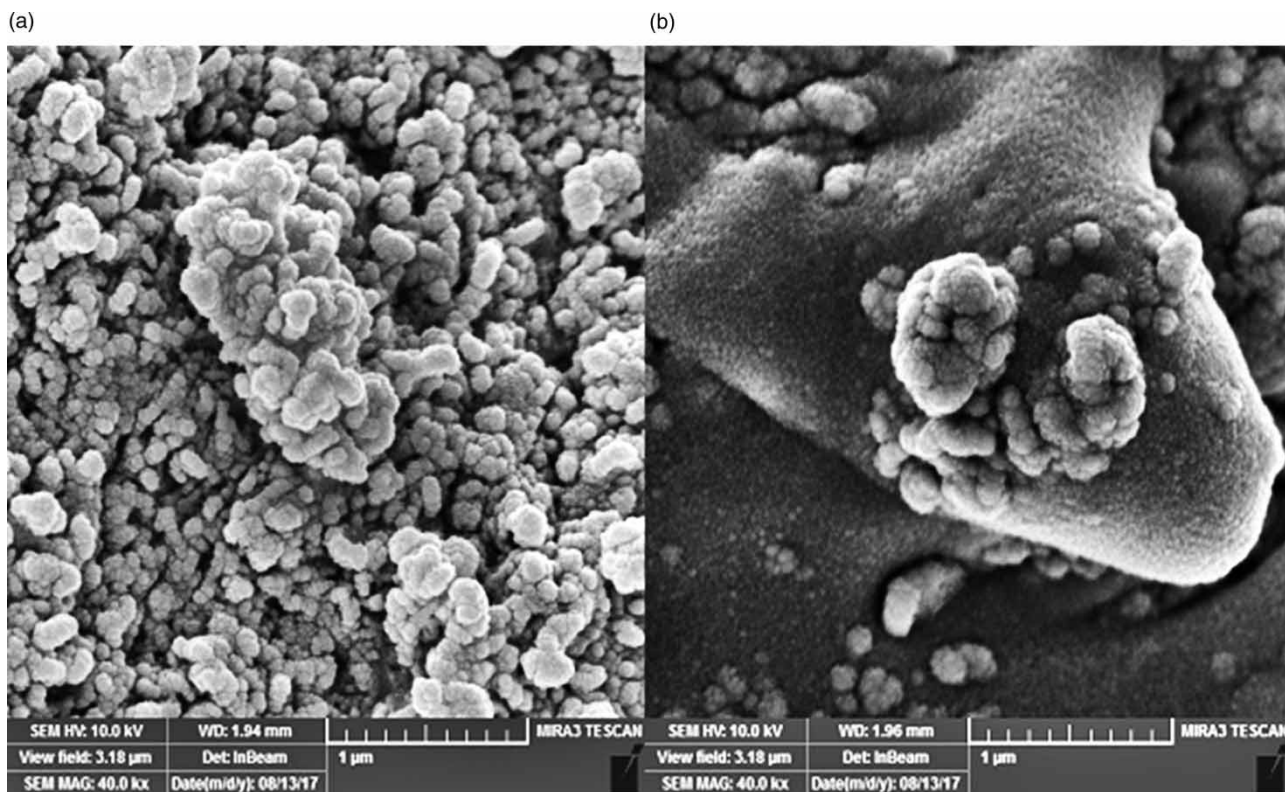
In this experiment, three samples were analyzed by FTIR spectroscopy. Figure 2(a) shows the spectrum of the first sample in which the produced sludge was analyzed in the absence of color contaminants. The absorption bands at wavenumbers 571 and 887  $\text{cm}^{-1}$  indicate the bending vibrations of Fe-O-H and Fe-O. Absorption bands centered near 1,638 and 3,428  $\text{cm}^{-1}$  are related to the tensile and flexural vibrations of the hydroxyl group, which confirm the presence of  $\text{Fe}(\text{OH})_3$ . The FTIR spectrum of the S.Y. dye pollutant is shown in Figure 2(b). The most obvious absorption band at the 1,193  $\text{cm}^{-1}$  wavelength is related to tensile vibrations (S=O). The absorption bands at 1,033 and 1,391  $\text{cm}^{-1}$  are related to the (C-N) and (C=C aromatic) vibrations, respectively. The absorption band at 1,391  $\text{cm}^{-1}$  is related to the C=C aromatic vibrations in the dye molecules. Naturally, because the S.Y. dye spectrum was prepared from its pure sample, the peak intensity will be higher. In the sample of sludge in the presence of the dye pollutant, as the amount of the dye concentration in the solution is in the range of ppm and the amount of contaminant adsorbed to the surface of the clots is very low, so the intensity of peaks is reduced. In the sample of sludge in the absence of contaminants, there was no dye at all with the sludge to observe the relevant peak. Figure 2(c) shows the spectrum of the sludge obtained from electrocoagulation in the presence of the dye pollutant. In this spectrum, almost all the adsorption bands related to the sludge are produced by the process, and the S.Y. dye pollutant is visible, which indicated that the pollutant had been adsorbed to the surface of the sludge and removed from the water.

### SEM and BET analysis

In this study, SEM imaging was performed on a sample of sludge. Figure 3(a) and 3(b) shows samples of the sludge produced in the process of electrocoagulation in the absence and presence of the dye contaminant. According to the images, the fine particles shown in both images are coagulant particles that adhere to the surface of the dye molecules (as shown in



**Figure 2** | FTIR spectrum of (a) sludge obtained the electrocoagulation process without the presence of dye pollutant, (b) Sunset Yellow dye pollutant, (c) sludge obtained by the electrocoagulation process in the presence of the dye pollutant.



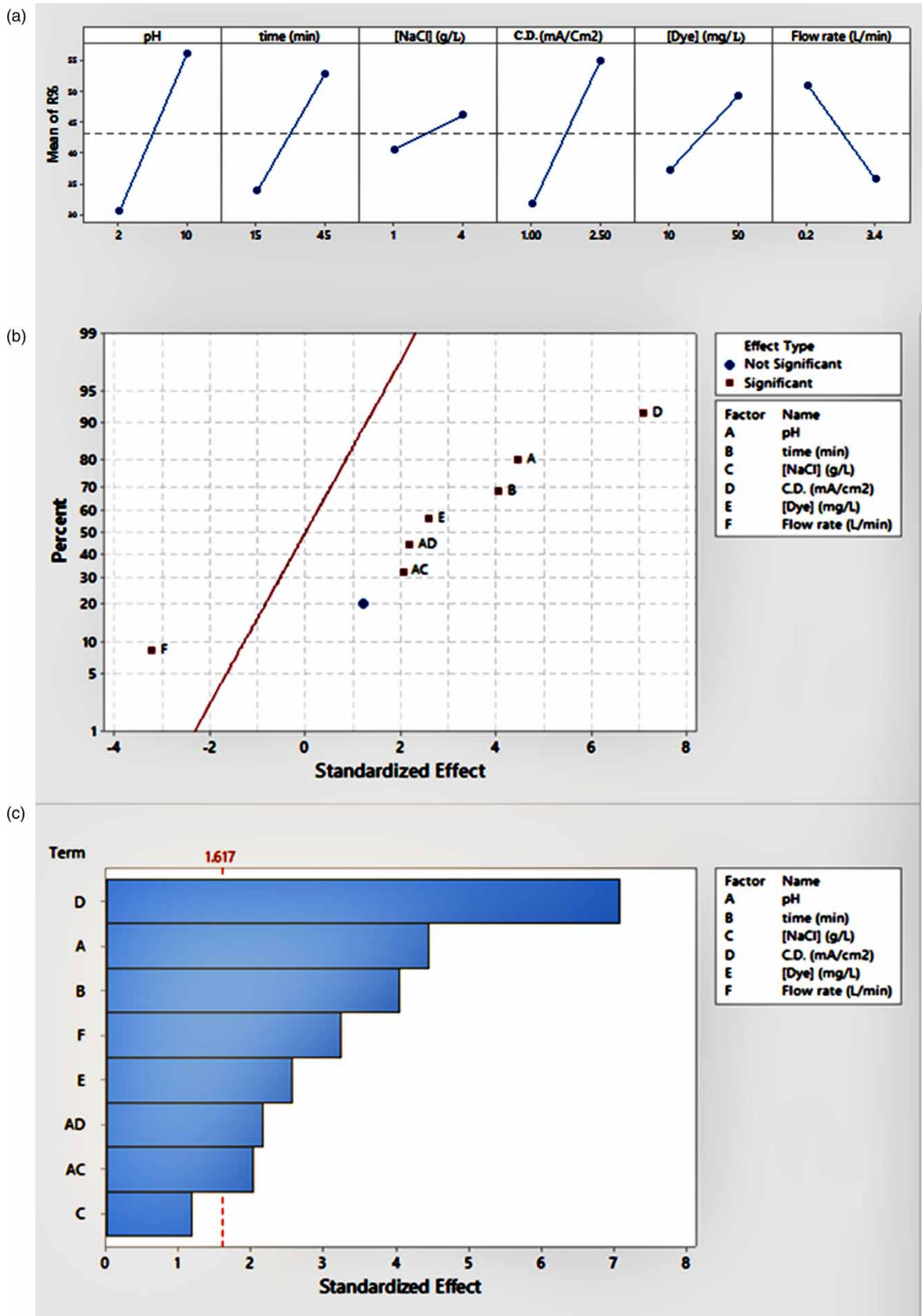
**Figure 3** | SEM images of sludge obtained the electrocoagulation process (a) without the presence of the dye pollutant, which is actually iron hydroxide, and (b) in the presence of the dye pollutant.

Figure 3(b)) and cause them to clot and precipitate. However, in the presence of colored contaminants, it was observed that large and heavy clots are formed, due to the adsorption of the contaminant molecules to the surface of the clots. According to the information obtained from BET analysis, the effective surface area of the particles forming the sludge was  $56.4073 \text{ m}^2/\text{g}$ . In this analysis, the total volume of the porosity of the sludge particles was equal to  $0.271222 \text{ cm}^3/\text{g}$ , and the average pore diameter was  $19.23131 \text{ nm}$ .

### Values of variables in screening tests

To optimize the dye removal process of S.Y. from contaminated water and to study the intensity of the parameters in the removal process, the present study examined several variables, including pH, the flow rate of solution, current density, initial dye concentration, reaction time, and electrolyte concentration using the Minitab software. The results in Figure 4(a) show that pH and current density are the most influential factors, and electrolyte concentration is the least effective parameter in this study. Therefore, in the process optimization studies, the electrolyte concentration was considered constant at a certain value ( $4 \text{ g/L}$ ), and other parameters were considered as the main process variables. In Figure 4(b), normal chart, as the data became closer to the base red line, the effect of the related parameter in the removal process decreases. In other words, whenever the distance of the point from the baseline increases, the factor is more effective in dye removal. In addition, the parameters indicated by the red square are considered effective parameters in the removal process, and the parameters indicated by the blue circle are among the ineffective factors in this process. As shown in Figure 4(b), the electrolyte concentration is the least effective, and the current density and pH are the most effective parameters in the process. The Pareto diagram, shown in Figure 4(c), also confirms the above results.

The residual diagrams, illustrated in Figure 5, are used for the adequacy analysis of the model. There are four assumptions to check adequacy, for example, data normality. As a statistical graph in the histogram chart, the Gaussian form of residual values indicates the normality of the statistical population. In addition, the data reveal suitable normality because there are numerous points around the central line of the normal probability distribution plot. The stability of variance is the next assumption



**Figure 4** | The mean range of R% and the effect of various parameters (a), parameters normal chart (b) and the screening test Pareto Chart in S.Y. dye removal (c).



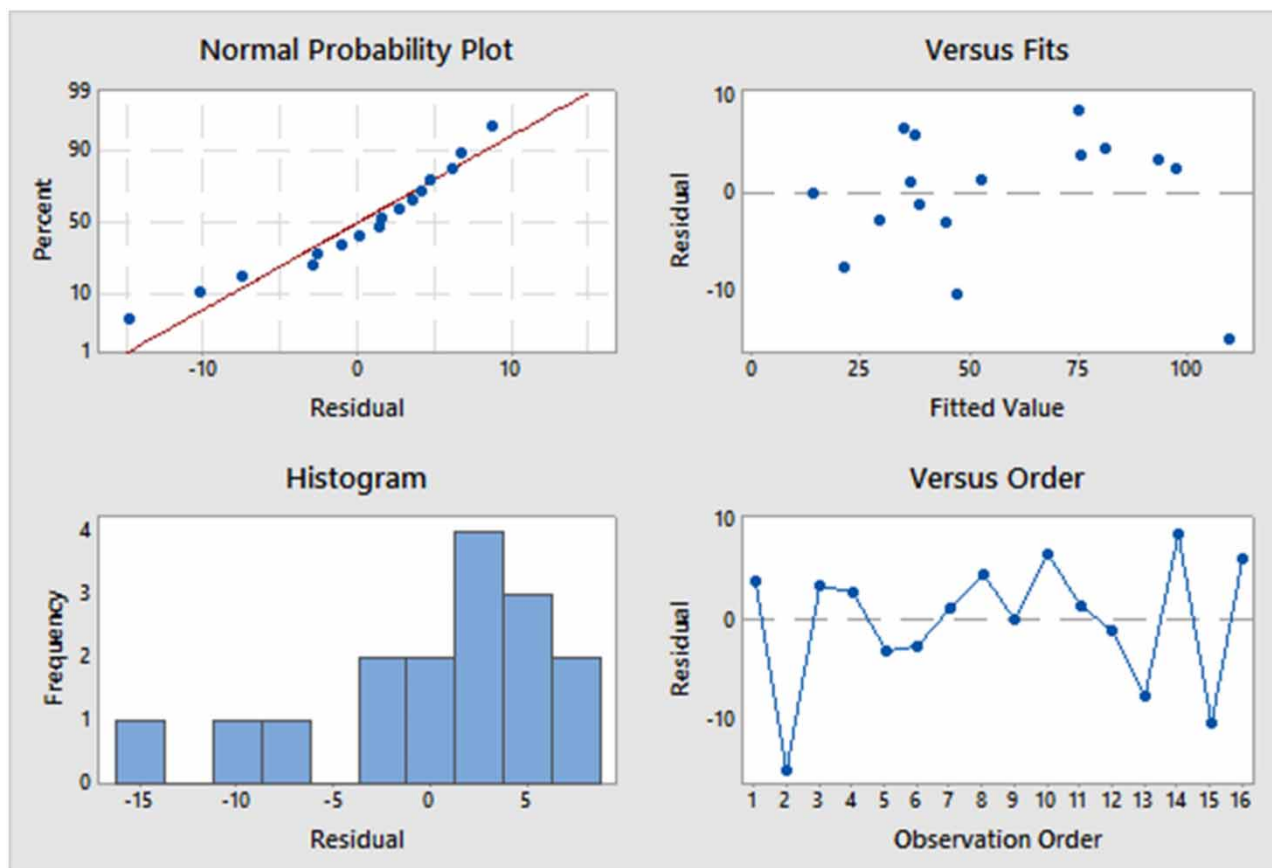


**Figure 5** | Residual diagrams to study the normality of data in S.Y. dye removal by the electrocoagulation process.

confirmed by the Versus Fits chart. When the residual data do not obey any particular pattern, the variance stability condition is satisfied. Similarly, the third adequacy assessment can be discussed by the use of the Versus Order diagram. The time independence of the data is defined as the parameter independent of time, and the mean and variance of the data do not change toward any special pattern. The Versus Order curve reveals that the residual alterations against the horizontal axis have no order, so time independence is obtained. In summary, Figure 5 proves the adequacy of the model; therefore, the data are normal.

### Data optimization and variable level determination

To examine the effect of the parameters on the screening domains more precisely, we distinguished each parameter in the screening range into five points. As a result, the accuracy of the test would increase within the specified period of the screening process. This section was also designed using Minitab software and included 33 experiments with two repetitions (Supplementary Material, Table S1). As shown in Figure 6(a), a higher curve slope shows a greater effect on the procedure. Thus, according to the previous results, the more influential factors are the pH and current density parameters. As can be seen in the diagram, the process time also has a high impact because the dye removal naturally increases as the reaction time lengthens. In addition, any parameter with a higher removal efficiency is more advantageous for the attainment of a higher dye removal percentage. Thus, a current density of about  $2.5 \text{ mA/cm}^2$ , a pH of 10, and a time of 45 minutes have the most optimal effect on the procedure. In terms of the time of electrolysis and current density, it was observed that by increasing the values of these parameters to more than the optimal value, the efficiency decreases, which seems to be due to excessive increase in clots and their collision with each other and desorption of pollutants from them. Also, the high amount of sludge produced in the solution may cover the surface of electrodes and prevent mass transfer, increase the electrical resistance of the electrochemical cell, and reduce efficiency. In the histogram in Figure 6(b), a Gaussian form exists, which proposes the normality of the data population, and proper accuracy of the results. Similarly, in the normal probability

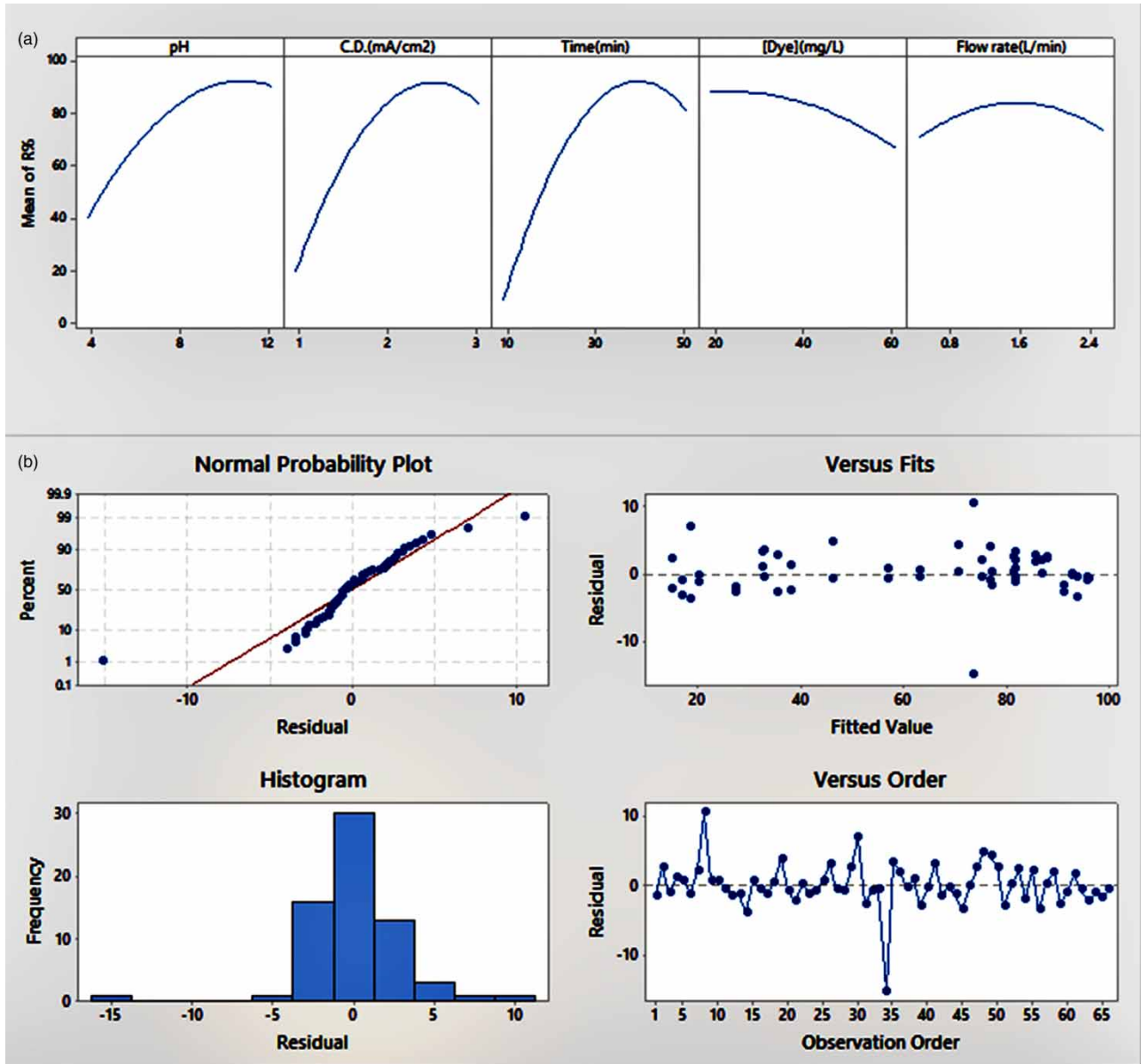


**Figure 6** | The efficiency study of parameters in S.Y. dye removal using the electrocoagulation method (a) and residual graphs for data accuracy examination (b).

plot, the points are distributed around the line properly, indicating the data normality. In addition, two other charts do not follow any specific pattern, so the high adequacy and correctness of the data are confirmed.

### Effects of operating parameters

The interaction of the parameters in the removal of S.Y. is shown in Figure 7. According to Figure 7, an increase in the initial dye concentration decreases the removal efficiency. This is because increasing the concentration of contaminants, as the speed and amount of clot production is constant and certain, gives rise to the decline in the removal efficiency. As the figures display, the removal efficiency increases with an increase in the flow rate of the solution to the reactor due to rapid sweeping of the hydrogen gas from the cathode surface and its non-accumulation on the electrode surface. Therefore, a reduction in the electrical resistance of electrochemical cells enhances the production of clots and the removal efficiency. Conversely, as the flow rate of the solution escalates, the contact of the dye molecules with the surface of the clots increases, which improves the performance of the system. It should be noted that when the flow rate of the solution exceeded the optimal value, the dye

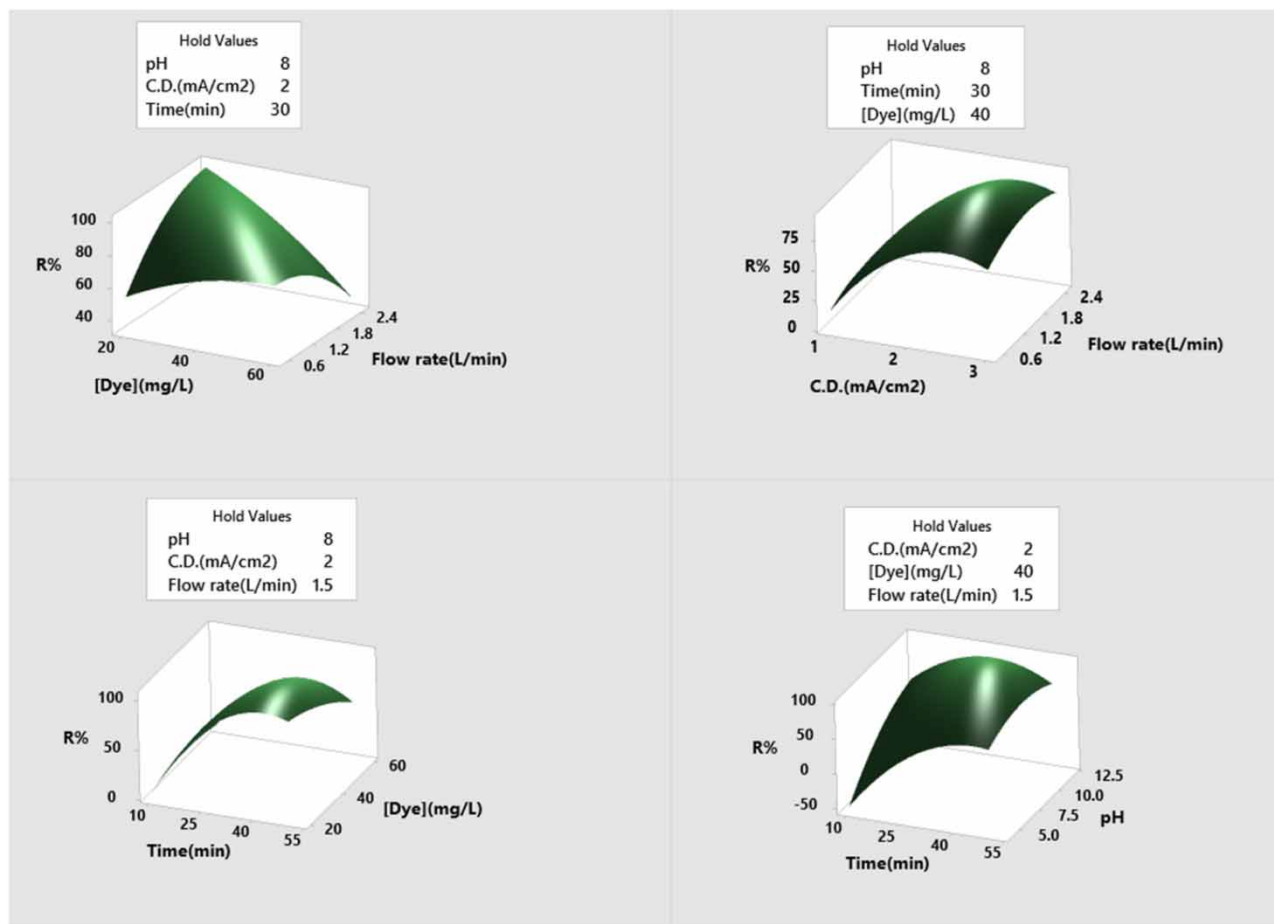


**Figure 7** | The effect of different parameters on the S.Y. dye removal using the electrocoagulation method.

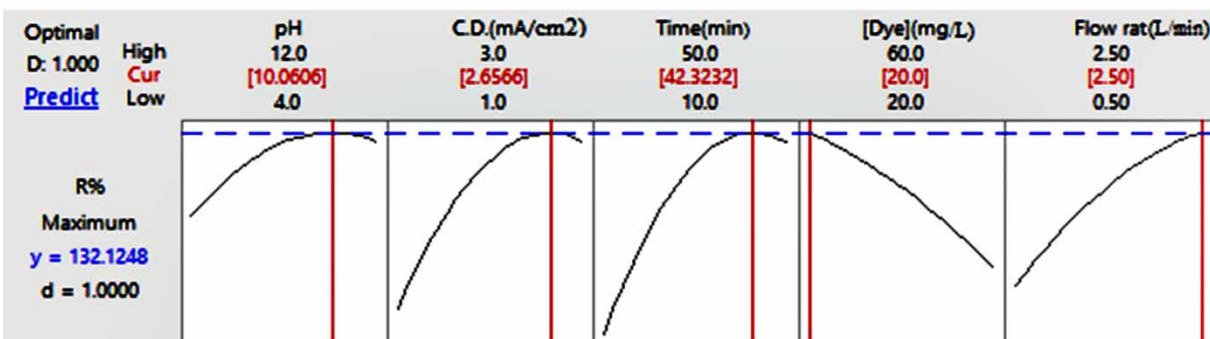
removal efficiency decreased due to an upsurge in system turbulence and desorption of the dye pollutants from the surface of the clots. As shown in Figure 7, as the current density enhanced, the removal efficiency increased due to the rise in the electrochemical reactions performed on the surface of the electrodes, resulting in an increase in the production of the iron hydroxide clots (Ntambwe Kambuyi *et al.* 2019). The results show that lengthening of the electrolysis time increased removal efficiency. Because longer periods increased the produced iron hydroxide this caused more removal of the pollutants. As Figure 7 shows, the dye removal efficiency increases with a rise in pH. As the pH changes, the species produced in the solution change as well. In an acidic medium, the iron hydroxide produced in the solution is dissolved, while, in a high pH, it converts to  $\text{Fe}(\text{OH})_4^-$ , which is also soluble. Therefore, with the reduction of the hydroxide clots, the removal of the color contaminants is also reduced (Chezeau *et al.* 2020). The most suitable pH in this process was about 9.

### Optimization results and regression equation

The Minitab software is able to introduce the values for each parameter as the best value to achieve the highest removal by reviewing the results of optimization tests. In fact, the purpose of designing an experiment in any way is to find the optimum conditions with the least amounts of time, cost, and energy. In Figure 8(a), to reach a 95% reliability, the software estimates the values of the parameters at the time of 42 min, pH of 10, current density of 2.65 mA/cm<sup>2</sup>, the flow rate of 2.5 L/min, and dye concentration of 20 mg/L. Using the mentioned values, over 100 and 99% removals were achieved in theory and practice, respectively. The theoretical removal efficiency of 132.12% indicates that this experiment has an extra capacity of 32.12% in removing the dye. The results are experimental and may differ about  $\pm 5\%$  tolerance from calculated values because of the 95% reliability in Minitab software.

By using a regression equation, the removal efficiency value can be obtained in the shortest time without performing an experiment according to the available values. Therefore, only by knowing the values of the parameters, the removal efficiency

(a)



(b)

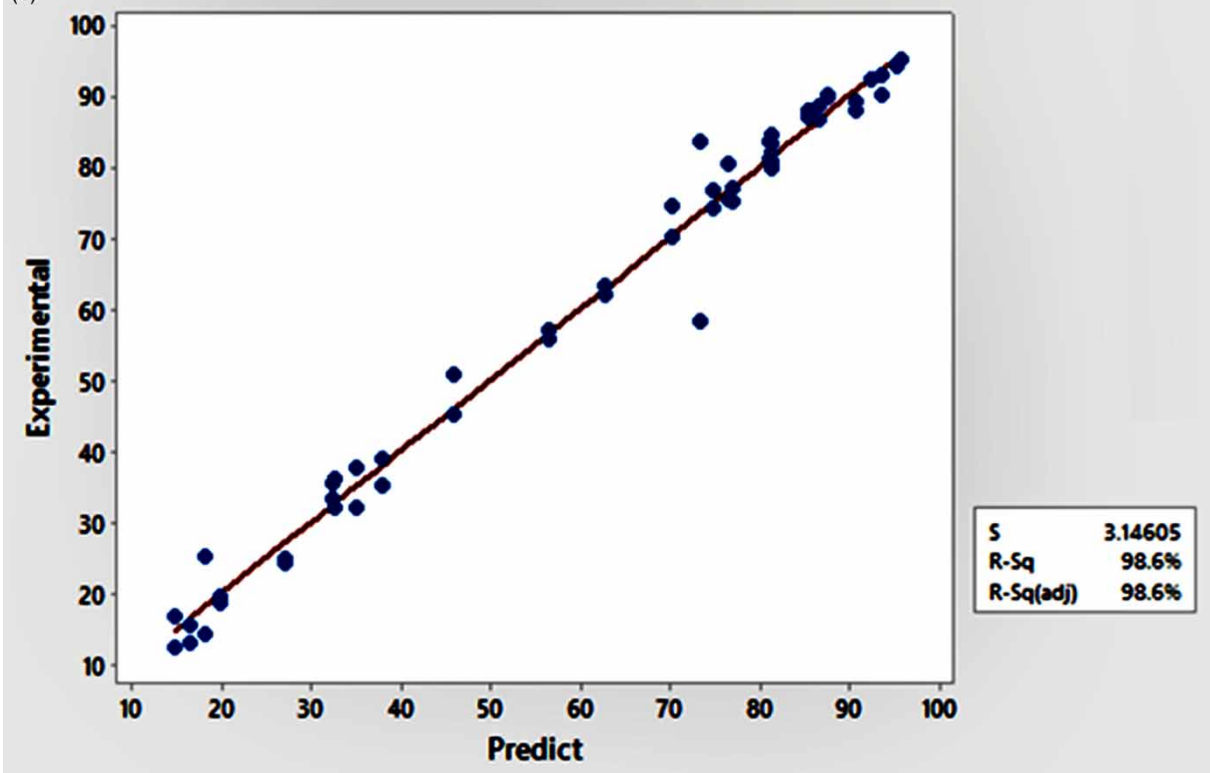


**Figure 8** | Prediction curves to optimize S.Y. dye removal using the electrocoagulation method (a) and regression graph of S.Y. dye removal by the electrocoagulation method (b).

can be easily calculated by the formula, although it should be noted that this formula was obtained after designing the optimization test. The regression equation is according to Equation (5).

$$\begin{aligned}
 R\% = & -357.7 + 13.80 X_1 + 104.7 X_3 + 9.748 X_2 + 1.680 X_4 + 42.1 X_5 - 1.053 X_1 \times X_1 \\
 & - 29.33 X_3 \times X_3 - 0.08914 X_2 \times X_2 - 0.01533 X_4 \times X_4 - 10.78 X_5 \times X_5 + 3.828 X_1 \times X_3 \\
 & - 0.2758 X_1 \times X_2 + 0.1545 X_1 \times X_4 + 2.291 X_1 \times X_5 + 0.047 X_3 \times X_2 + 0.168 X_3 \times X_4 \\
 & + 2.76 X_3 \times X_5 - 0.02916 X_2 \times X_4 + 0.399 X_2 \times X_5 - 1.112 X_4 \times X_5
 \end{aligned}
 \tag{5}$$

where  $X_1$ ,  $X_2$ ,  $X_3$ ,  $X_4$  and  $X_5$  indicate pH, time of electrolysis (min), current density ( $\text{mA}/\text{cm}^2$ ), dye concentration ( $\text{mg}/\text{L}$ ), and flow rate ( $\text{L}/\text{min}$ ), respectively. Figure 8(b) confirms the accuracy of the optimization tests. As can be seen, fewer errors occurred when the predicted values were closer to the experimental amounts, which means placing of the points on the line. So, the experimental data distribution was close to the predicted values of the software, and the fewest operator/device errors are obtained.

## CONCLUSION

To remove the S.Y. dye pollutant, the present study used an electrocoagulation method, an electrochemical reactor with concentric electrodes, and the RSM and obtained an efficiency of  $>99\%$ , which indicated the high efficiency of this method for the removal of S.Y. from contaminated water. According to the obtained results, we can argue that the most important parameters for achieving a high removal efficiency are pH and current density. Using the results of screening experiments, electrolyte concentration was the least effective parameter, so in this study we considered the concentration of the sodium chloride electrolyte at a constant value of  $4 \text{ g}/\text{L}$  and studied the other parameters in 66 experiments according to the optimization program of the RSM. Furthermore, the RSM was optimized, and the best conditions for the S.Y. dye removal process were a time of 42 min, a pH of 10, a current density of  $2.65 \text{ mA}/\text{cm}^2$ , a flow rate of  $2.5 \text{ L}/\text{min}$ , and dye concentration of  $20 \text{ mg}/\text{L}$ . Using Minitab software, we could predict a 100% efficiency by the RSM in the optimal conditions. Results showed that with increase in current density, time of electrolysis and flow rate of solution, the dye removal efficiency increased, but the dye removal efficiency decreased with a rise in dye concentration. SEM images and FTIR analyses indicated that, in this process, the S.Y. pollutant was adsorbed to the surface of the sludge and removed from the water.

## ACKNOWLEDGEMENTS

We would thank from the Tabriz branch of Islamic Azad University for their guidance and financial supports.

## DATA AVAILABILITY STATEMENT

All relevant data are included in the paper or its Supplementary Information.

## REFERENCES

- Arnold, L. E., Lofthouse, N. & Hurt, E. 2012 Artificial food colors and attention-deficit/hyperactivity symptoms, conclusions to dye for. *Neurotherapeutics* **9**, 599–609. doi: 10.1007/s13311-012-0133-x.
- Bendaia, M., Hazourli, S., Aitbara, A. & Merzoug, N. 2021 Performance of electrocoagulation for food azo dyes treatment in aqueous solution: optimization, kinetics, isotherms, thermodynamic study and mechanisms. *Separation Science and Technology* **56**, 2087–2103.
- Bracher, G. H., Carissimi, E., Wolff, D. B., Graepin, C. & Hubner, A. P. 2021 Optimization of an electrocoagulation-flotation system for domestic wastewater treatment and reuse. *Environmental Technology* **42**, 2669–2679.
- Chelladurai, S. J. S., Murugan, K., Ray, A. P., Upadhyaya, M., Narasimharaj, V. & Gnanasekaran, S. 2021 Optimization of process parameters using response surface methodology: a review. *Materials Today: Proceedings* **37**, 1301–1304.
- Chezeau, B., Boudriche, L., Vial, C. & Boudjemaa, A. 2020 Treatment of dairy wastewater by electrocoagulation process: advantages of combined iron/aluminum electrodes. *Separation Science and Technology* **55**, 2510–2527.
- Deepika, S., Harishkumar, R., Dinesh, M., Abarna, R., Anbalagan, M., Roopan, S. M. & Selvaraj, C. I. 2017 Photocatalytic degradation of synthetic food dye, sunset yellow FCF (FD&C yellow no. 6) by *Ailanthus excelsa* Roxb. possessing antioxidant and cytotoxic activity. *Journal of Photochemistry and Photobiology B: Biology* **177**, 44–55.
- Elami, D. & Seyyedi, K. 2020 Removing of carmoisine dye pollutant from contaminated waters by photocatalytic method using a thin film fixed bed reactor. *Journal of Environmental Science and Health, Part A* **55**, 193–208.
- Gao, H., Zhang, L. & Liao, Y. 2016 Removal of sunset yellow FCF from aqueous solution using polyethyleneimine-modified MWCNTs. *Water Science and Technology* **73**, 1269–1278.
- Garajehdaghi, M. & Seyyedi, K. 2019 Removing of the dye pollutant acid red 1 from contaminated waters by electrocoagulation method using a recirculating tubular reactor with punched anode. *Journal of the Chemical Society of Pakistan* **41**, 191–197.
- Gautam, K., Kamsonlian, S. & Kumar, S. 2020 Removal of Reactive Red 120 dye from wastewater using electrocoagulation: optimization using multivariate approach, economic analysis, and sludge characterization. *Separation Science and Technology* **55**, 3412–3426.
- Ghaffarian Khorram, A. & Fallah, N. 2018 Treatment of textile dyeing factory wastewater by electrocoagulation with low sludge settling time: optimization of operating parameters by RSM. *Journal of Environmental Chemical Engineering* **6**, 635–642.
- Gomes, A. J., Das, K. K., Jame, S. A. & Cocke, D. L. 2016 Treatment of truck wash water using electrocoagulation. *Desalination and Water Treatment* **57**, 25991–26002.

- Hanay, O. & Hasar, H. 2011 Effect of anions on removing  $\text{Cu}^{2+}$ ,  $\text{Mn}^{2+}$  and  $\text{Zn}^{2+}$  in electrocoagulation process using aluminum electrodes. *Journal of Hazardous Materials* **189**, 572–576.
- Kashefialasl, M., Khosravi, M., Marandi, R. & Seyyedi, K. 2005 Treatment of dye solution containing colored index acid yellow 36 by electrocoagulation using iron electrodes. *International Journal of Environmental Science and Technology* **2**, 365–371.
- Khadivi, S. M., Edjlali, L., Akbarzadeh, A. & Seyyedi, K. 2019 Enhanced adsorption behavior of amended EDTA–graphene oxide for methylene blue and heavy metal ions. *International Journal of Environmental Science and Technology* **16**, 8151–8160.
- Khoshbin, S. & Seyyedi, K. 2017 Removal of acid red 1 dye pollutant from contaminated waters by electrocoagulation method using a recirculating tubular reactor. *Latin American Applied Research* **47**, 101–105.
- Liu, Y., Wang, P., Gojenko, B., Yu, J., Wei, L., Luo, D. & Xiao, T. 2021 A review of water pollution arising from agriculture and mining activities in Central Asia: facts, causes and effect. *Environmental Pollution* **291**, 118209.
- Lu, J., Zhang, P. & Li, J. 2021 Electrocoagulation technology for water purification: an update review on reactor design and some newly concerned pollutants removal. *Journal of Environmental Management* **296**, 113259.
- Mook, W. T., Aroua, M. K., Szlachta, M. & Lee, C. S. 2017 Optimisation of reactive black 5 dye removal by electrocoagulation process using response surface methodology. *Water Science & Technology* **75**, 952–962.
- Naresh Yadav, D., Anand Kishore, K. & Saroj, D. 2021 A study on removal of Methylene Blue dye by photo catalysis integrated with nanofiltration using statistical and experimental approaches. *Environmental Technology* **42**, 2968–2981.
- Nippatlapalli, N. & Philip, L. 2020 Assessment of novel rotating bipolar multiple disc electrode electrocoagulation–flotation and pulsed plasma corona discharge for the treatment of textile dyes. *Water Science and Technology* **81**, 564–570.
- Ntambwe Kambuyi, T., Eddaqaq, F., Driouich, A., Bejjany, B., Lekhlif, B., Mellouk, H., Digua, K. & Dani, A. 2019 Using response surface methodology (RSM) for optimizing turbidity removal by electrocoagulation/electro-flotation in an internal loop airlift reactor. *Water Supply* **19**, 2476–2484.
- Sahu, O., Mazumdar, B. & Chaudhari, P. K. 2014 Treatment of wastewater by electrocoagulation: a review. *Environmental Science and Pollution Research* **21**, 2397–2413.
- Seyyedi, K. & Mahdiyar, A. 2015 Decolorization of contaminated water containing C.I. Direct blue 53 by macroalgae *Chara* sp. and optimization of decolorization process. *Latin American Applied Research* **45**, 193–198.
- Sires, I. & Brillas, E. 2012 Remediation of water pollution caused by pharmaceutical residues based on electrochemical separation and degradation technologies. *Environment International* **40**, 212–229.
- Syam Babu, D., Anantha Singh, T. S., Nidheesh, P. V. & Suresh Kumar, M. 2020 Industrial wastewater treatment by electrocoagulation process. *Separation Science and Technology* **55**, 3195–3227.
- Xu, J., Du, Y., Qiu, T., Zhou, L., Li, Y., Chen, F. & Sun, J. 2021 Application of hybrid electrocoagulation–filtration methods in the pretreatment of marine aquaculture wastewater. *Water Science and Technology* **83**, 1315–1326.

First received 21 September 2021; accepted in revised form 5 November 2021. Available online 18 November 2021